Orientation-Selective Incorporation of Transmembrane F_0F_1 ATP Synthase Complex from *Micrococcus luteus* in Polymer-Supported Membranes

Murat Tutus, Fernanda F. Rossetti, Emanuel Schneck, Giovanna Fragneto, Friedrich Förster, Ralf Richter, Thomas Nawroth, Motomu Tanaka*

We report the vectorial incorporation of a highly asymmetric F_0F_1 ATP synthase complex from *Micrococcus luteus* into polymer-supported membranes. Dynamic light scattering and cryo electron microscopy confirm that the use of weak surfactants (bile acid) allows for the non-disruptive protein incorporation into lipid vesicles. Spreading of vesicles with ATP synthase onto a cellulose support results in a homogeneous distribution of proteins, in contrast to a patchy image observed on bare glass slides. The orientation of ATP synthase can be identified using an antibody to the ATP binding site as well as from topographic profiles of the surface. The method to "align" transmembrane proteins in supported membranes would open a possibility to quantify protein functions in biomimetic model systems.

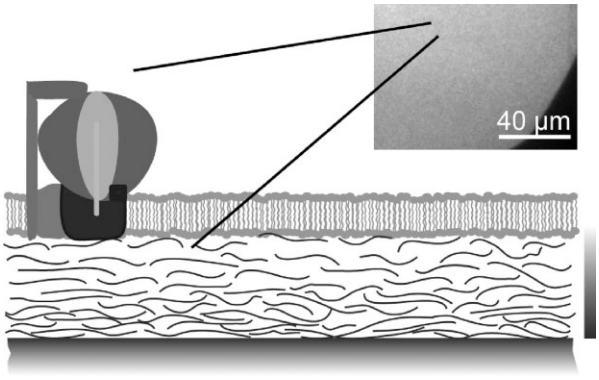

M. Tutus, F. F. Rossetti, E. Schneck, R. Richter, M. Tanaka
Biophysical Chemistry Laboratory and Center for Quantitative Biology (BIOQUANT), University of Heidelberg, 69120 Heidelberg, Germany
E-mail: tanaka@uni-heidelberg.de
M. Tutus, F. F. Rossetti, E. Schneck, T. Nawroth, M. Tanaka
Department of Physics, Technical University of Munich, D85748 Garching, Germany
G. Fragneto
Institut Laue-Langevin, F38043 Grenoble Cedex, France
F. Förster
Department of Molecular Structural Biology, Max Planck Institute for Biochemistry, 82152 Martinsried, Germany
R. Richter
Current address: Biosurfaces Unit, CIC biomaGUNE, 20009 San Sebastian, Spain
T. Nawroth
Current address: Institute of Pharmacy, University of Mainz, Staudingerweg 5, 55099 Mainz, Germany

Introduction

Biological membranes are vital components that define the outer boundary of living cells and organelles. They consist largely of a lipid bilayer and membrane-associated proteins that facilitate specific recognition on the membrane and material transport across the membrane. To bypass the structural complexity of biological membranes and their dynamic interactions with intra- and extracellular networks, artificial model membranes have played an important role in unraveling the physical and chemical characteristics of membranes and the resulting biological functions. Among various model membranes, phospholipid bilayers deposited onto solid substrates (so-called solid supported membranes) have been the most widely used

Macromol. Biosci. **2008**, *8*, 1034–1043

DOI: 10.1002/mabi.200800128

experimental cell surface model.[1–3] Their lateral fluidity and stability on planar surfaces offer distinct advantages over other model membranes to apply physical characterization methods such as total interference fluorescence,[4] NMR[5] and FT-IR spectroscopy,[6] surface plasmon resonance,[7] quartz crystal microbalance,[8] and neutron reflectivity.[9]

A common approach to functionalize supported membranes with transmembrane proteins (such as ion channels or receptors) is to spread vesicles incorporating proteins (proteoliposomes) onto planar supports. However, solid supported membranes have some fundamental drawbacks. In particular, the thickness of the water gap between the membrane and the solid surface is not sufficiently large to avoid direct contact of transmembrane proteins with the solid surface. This problem can be avoided by separating the membrane from the solid substrate using soft polymeric materials that rest on the substrate and support the membrane (so-called polymer-supported membranes).[10,11] To date, we demonstrated that the presence of polymer interlayers with a thickness of 5–10 nm significantly improves the homogeneity, lateral diffusivity, and function of transmembrane receptors, such as human platelet integrin.[12–16] Transmembrane proteins are often incorporated into lipid vesicles from micelles of detergents, such as Triton X-100 that has a low critical micelle concentration (cmc $\approx 0.3 \cdot 10^{-3}$ M). This process often leads to the disruption of membranes, which results in the random protein orientation in vesicles with broad size distribution (Figure 1, left).[12]

In this study, we use a bile acid, taurodeoxycholate (TDOC), whose cmc is about $3 \cdot 10^{-3}$ M. As previously demonstrated by Nawroth et al. using neutron scattering,[17] TDOC can be incorporated into phospholipids vesicles at lower concentrations ($1.5 \cdot 10^{-3}$ M, about 5 mol-% of lipids) without causing membrane disruption (Figure 1, right). Moreover, due to its larger cmc, such bile acids can be removed more easily than Triton X-100 simply by size exclusion chromatography. As the target protein, we choose F_0F_1 ATP synthase complex purified from *Micrococcus luteus*. ATP synthase consists of a F_1 head group with a diameter of about 10 nm and a transmembrane F_0 part (5 nm in diameter) connected by a flexible transmission and a rigid second stalk, which form one of the largest asymmetric complex structures that have ever been resolved.[18–20] In *Micrococcus luteus*, the F_1 head group contains 5 subunits and the F_0 part is made out of 3 subunits. The molecular weight (MW) of the ATP synthase from *Micrococcus luteus* is estimated to be about 550 kDa as the following: Electrophoresis with concentration variations suggests that the MW of a F_1 head group is 412 kDa (error: ±5%). Thus, assuming the actual stoichiometry of the F_0 group as ab_2c_{12}, the MW of a complete enzyme complex can be determined either by Lämmli gels

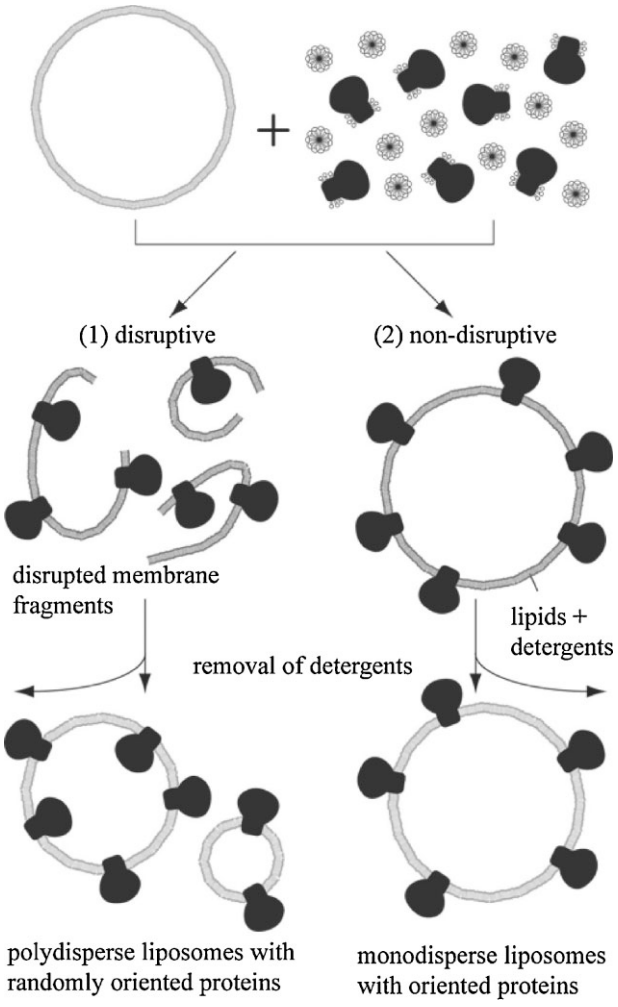

Figure 1. Disruptive (left) and non-disruptive (right) reconstitutions of asymmetric transmembrane proteins in lipid vesicles.

(558 kDa) or Schägger gels (522 kDa). Here, we incorporate ATP synthase into lipid vesicles of well-defined size, and verify non-disruptive reconstitution of proteins by measuring the size distributions of vesicles before and after protein incorporation. The bulky F_1 head group can be used as a marker to confirm the reconstitution of the entire complex using cryo electron microscopy and atomic force microscopy (AFM). To judge if the incorporated ATP synthase retains its natural functions, we apply the antibodies that bind specifically to the ATP binding site.

Experimental Part

Chemicals, Lipids

Unless stated otherwise, all chemicals were purchased from Sigma Aldrich (Taufkirchen, Germany) and used without further purification. Deionized ultra pure water (Millipore, Molsheim,

France) with a specific resistance of $R > 18$ M$\Omega \cdot$cm^{-1} and tris-(hydroxymethyl)-aminoethane (TRIS) buffer ($50 \cdot 10^{-3}$ M TRIS, $5 \cdot 10^{-3}$ M $MgCl_2$, $2 \cdot 10^{-3}$ M acid, pH = 8) were used throughout the study. 1-Stearoyl-2-oleyl-*sn*-glycero-3-phosphatidylcholin (SOPC) and 1-oleoyl-2-{12-[(7-nitro-2-1,3-benzoxadiazol-4-yl)amino]dodecanoyl}-*sn*-glycero-3-phosphocholine (NBD-PC) were purchased from Avanti Polar Lipids (Alabaster, USA).

F_0F_1 ATP Synthase from *Micrococcus luteus*

F_0F_1 ATP synthase was purified from the air and sunlight resistant bacterium *Micrococcus luteus* ATCC 4698 in remarkably stable form (>2 d at 20 °C) as described elsewhere[21,22] by improvement of the early isolation according to Chung and Salton.[23] Proteins were pre-extracted with 3-[(3-chlamidopropyl) dimethylammonio]-1-propanesulfonate, followed by the extraction with Triton X-100. Triton X-100 was then replaced by taurodeoxycholate (TDOC). The stock solution was buffered by $50 \cdot 10^{-3}$ M tris-(hydroxymethyl)-aminoethane (pH = 8) containing $0.1 \cdot 10^{-3}$ M diisopropyl fluorophosphate (DFP) and 10 vol.-% glycerol. For storage, the samples were deep-frozen in liquid nitrogen.

For the chemical (and thus nonspecific) labeling of ATP synthase, 5-(and-6)-carboxytetramethylrhodamine succinimidyl ester [5(6) TAMRA-SE] from Molecular Probes (Leiden, Netherlands) was coupled to proteins according to the methods used for other transmembrane proteins.[12,24] The efficiency of the fluorescence labeling was determined by normalizing the concentration of TAMRA by the total protein concentration. Taking the extinction coefficient of ATP synthase, $\varepsilon = 250\,000$ L$\cdot$mol$^{-1}\cdot$cm^{-1},[25] the protein concentration of $0.2 \cdot 10^{-6}$ M was estimated. The concentration of TAMRA of $2.2 \cdot 10^{-6}$ M could be estimated by the adsorption peak at $\lambda = 555$ nm, corresponding to 9 dyes per protein. On the other hand, the specific immuno-labeling of ATP synthase entailed some difficulties due to the fact that the complete amino acid sequence of ATP synthase from *Micrococcus luteus* is yet unknown. However, since the amino acid sequence of the ATP binding site of β subunit has high homologies among various organisms, we took the first monoclonal antibody against β subunit of ATP synthase from rat brain mitochondria (Chemicon, Temecula, USA). The specificity of the first monoclonal antibody was tested by applying the second polyclonal goat anti-mouse IgG conjugated with fluorescein isothiocyanate (FITC, Sigma Aldrich, Taufkirchen, Germany). To avoid nonspecific binding of antibodies, the membrane was treated with 3 wt.-% bovine serum albumin (BSA, Sigma Aldrich, Taufkirchen, Germany) for 1 h.

Substrates, Cellulose Supports

Glass slides were purchased from Karl Hecht KG (Assistent, Sondheim, Germany). Single-side polished silicon (111) blocks ($80 \times 50 \times 15$ mm^3) for the neutron reflectivity experiments were purchased from Siliciumbearbeitung Holm (Tann, Germany). Both the glass slides and the silicon blocks were cleaned by sonicating them with acetone, ethanol, methanol, deionized water and immersing them into a solution of 1:1:5 (by volume) H_2O_2 (30%): NH_4OH (30%): H_2O for 5 min. at room temperature, before soaking them for another 30 min at 60 °C. Afterwards, they were intensively rinsed with deionized water, dried at 70 °C, and stored in sealed glass boxes.

Prior to the deposition of cellulose films, all substrates were hydrophobized with octadecyltrimetoxysilane (ODTMS), purchased from ABCR (Karlsruhe, Germany).[26] Trimethylsilylcellulose (TMSC) was synthesized from cellulose powder (MW $\approx$ 25 kDa, purchased from Fluka), as previously reported.[27,28] The degree of substitution (D.S.) was estimated by elemental analysis to be D.S. = 2.1. The stock solution of TMSC (in chloroform) was spread on the water subphase of a self-built Langmuir trough at 20 °C, and compressed to a surface pressure of 30 mN$\cdot$m^{-1}. The surface pressure was kept constant throughout the successive Langmuir-Blodgett deposition of 10 monolayers onto the hydrophobized substrates. The hydrophobic trimethylsilyl side chains were cleaved by exposing the film to the vapor of concentrated HCl for 20 s, resulting in a hydrophilic, regenerated cellulose film.

Neutron Reflectivity

Neutron specular reflectivity experiments were carried out in time-of-flight (TOF) mode at the D17 beamline[29] of the Institut Laue Langevin (ILL) in Grenoble (France). The cellulose film deposited on silicon blocks were measured first in air and subsequently under D_2O. The obtained data was binned to reduce the statistic errors and fitted with the programs Motofit[30] and Parratt32[31] using either a box model (in the case of dry cellulose), or a combination of a decay (stretched exponential) profile function (for the hydrated cellulose layer) and a box model (for the underlying layers).

Reconstitution of ATP Synthase in Liposomes

A solution of SOPC dissolved in chloroform was dried in a rotary evaporator, and placed in vacuum overnight. The dried lipids were dispersed in $50 \cdot 10^{-3}$ M TRIS buffer (pH = 8) at a concentration of 1 mg$\cdot$mL^{-1}, incubated at 50 °C for 2 h, which resulted in multilamellar liposomes. To obtain single unilamellar liposomes with a distinct size, the liposome suspension was extruded 31 times through two porous polycarbonate filters with a pore radius of 25 or 50 nm (LiposoFast Extruder, Avestin Inc., Ottawa, Canada). Single unilamellar liposomes were incubated with ATP synthase stabilized with TDOC for 30 min at room temperature. After the incubation, TDOC was removed by a gel permeation chromatography (GPC) column filled with Sephadex G 25 (Amersham Pharmacia Biotech AB, Uppsala, Sweden) as described previously.[21,22]

Dynamic Light Scattering (DLS)

The size of lipid vesicles before and after protein incorporation was determined by DLS. All measurements were carried out at room temperature. The samples were illuminated by a laser light ($\lambda = 632.8$ nm), and the scattered light was detected by a single photon detection unit that was connected to a correlator (ALV5000/E, Langen, Germany) at an angle of 170° with respect to the incident beam. A series of solutions that fit the data are computed with CONTIN software,[32] and the obtained histograms were analyzed with a self-written fitting routine.

Macromolecular Journals
DOI: 10.1002/mabi.200800128

Cryo Electron Microscopy

Cryo electron microscopy was performed on a Philips CM 120 Biofilter (Philips E.O., Eindhoven, Netherlands) with a post column energy filter.[33,34] The experiments were carried out at the acceleration voltage of 120 kV and the magnification of 3.1×10^4 times. A holey carbon grid (Quantifoil Micro Tools GmbH, Jena, Germany) was rendered hydrophilic by plasma cleaning, and a 10 μL portion of vesicle suspension was applied onto the grid. The grid was vitrified in liquid ethane without applying any contrast method and assembled under liquid nitrogen into a cooled specimen holder. The sample was transferred into the electron microscope and illuminated by low irradiation doses ($\leq$100 electrons $\cdot$ nm^{-2}) for recording high resolution images of radiation-sensitive specimen.

Spreading of Proteoliposomes, Fluorescence Imaging

Proteoliposomes were spread on the cellulose film and incubated at 37 °C for 1 h. The homogeneity of the supported membranes and reconstituted ATP synthase was verified using an inverted microscope (Axiovert 200, Carl Zeiss, Göttingen, Germany), equipped with a 63 × long distance objective (n.a. 0.75) and filter sets for the used dyes. The images taken by a cooled CCD camera (Orca ER, Hamamatsu Photonics, Hersching, Germany) were digitized by a frame-grabber-card (Stemmer Imaging, Puchheim, Germany) and processed by a self-developed software. The lipid membrane was labeled by doping 1 mol-% of NBD-PC into proteoliposomes, while ATP synthase in the membrane was labeled either by non-specific coupling of TAMRA or by immunofluorescence labeling with antibodies.

Atomic Force Microscopy (AFM)

The topography of the polymer supported membrane was characterized with an atomic force microscope (NanoWizard, JPK Instruments, Berlin, Germany). Silicon [100] wafers, coated with thermal oxide (1×1 cm^2), were chosen as solid supports. The contact mode fluid cell as well as the cantilever were cleaned and mounted together. Using a double-sided tape (TESA, Hamburg, Germany) the specimen were attached to a custom-made sample holder. Proteoliposomes were added onto the specimen, incubated for 1 h, and rinsed extensively with buffer. After the installation of the AFM scanner, the system was equilibrated for 30 min. Contact mode images were acquired at a scan rate of 8 Hz.

Results and Discussion

DLS

After removing the remaining TDOC from the proteoliposomes with GPC, the concentration of ATP synthase of $0.2 \cdot 10^{-6}$ M can be determined from the adsorption peak at $\lambda = 280$ nm in the extinction spectra. The lipid concentration of $1.1 \cdot 10^{-3}$ M can be measured by phosphate analysis.[35] Considering the large size difference between liposomes and TDOC micelles,[36] the obtained results confirmed the incorporation of ATP synthase into lipid vesicles.

To verify the non-disruptive incorporation of ATP synthase into liposomes without disruption, the size distribution of liposomes before and after protein incorporation is quantitatively determined using dynamic light scattering. Figure 2 shows the number weighted size distributions of liposomes and proteoliposomes. The histogram of liposomes extruded through a porous filter (in this experiment, the one with a pore radius of 25 nm) shows an asymmetric broadening towards the larger size, which can be analyzed with the Weibull distribution:[37]

$$y = y_0 + A\left[\frac{w_2 - 1}{w_2}\right]^{\frac{1-w_2}{w_2}} [S]^{w_2 - 1} \exp[-S]^{w_2} + \left[\frac{w_2 - 1}{w_2}\right] \quad (1)$$

As presented in Figure 2, the histogram of intact liposomes (solid squares) can be well fitted with the Weibull distribution (solid line), yielding a peak position corresponding to the radius of 31.8 nm and a full width at half maximum (FWHM) of 12.9 nm. The incubation of liposomes with TDOC-stabilized ATP synthase and the removal of the TDOC with GPC cause almost no change in the size distribution of liposomes (open circles). Indeed,

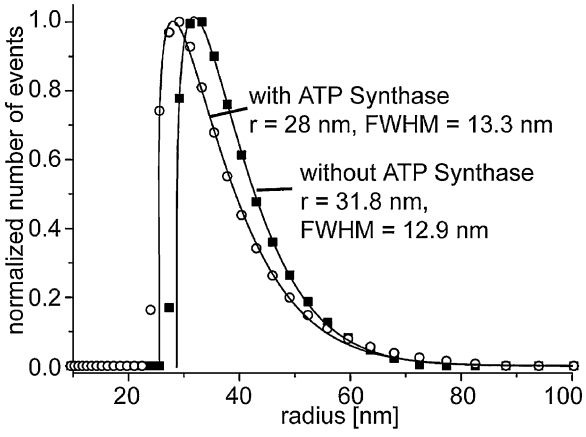

Figure 2. Number-weighted size distribution of hydrodynamic radii of SOPC vesicles extruded through pore radius of $r = 25$ nm, presented by solid squares (■). The corresponding results from the same liposomes after reconstitution of ATP synthase are given as open circles (○). Both of the obtained histograms can be well analyzed with the Weibull distribution yielding a radius of 31.8 nm and a FWHM of 12.9 nm for SOPC liposomes and 28.0 nm and 13.3 nm for ATP synthase proteoliposomes. Almost identical size distributions before and after protein incorporation imply the non-disruptive incorporation of ATP synthase (Figure 1, left).

the peak position (28.0 nm) and width (FWHM = 13.3 nm) of the proteoliposomes gained from the same fitting routine (solid line) are almost identical to those of intact liposomes.

The obtained results clearly indicate that the incorporation of transmembrane proteins (ATP synthase) into preformed liposomes in the presence of TDOC does not cause the disruption or fusion of liposomes. The fact that we observed no remarkable influence of the incorporated proteins on the measured size distribution can be attributed to the relatively small number of proteins in each liposome. If one takes the molar ratio between proteins and lipids (1:5 000), the mean molecular area of lipid (0.7 nm^2) and the cross sectional area of the transmembrane part of ATP synthase (20 nm^2), one can assume that about six proteins are incorporated in each liposome. Thus, it seems reasonable that the incorporation of the proteins caused almost no change in the size distribution. This finding agrees well with previous studies, where we reported the vectorial incorporation of ATP synthase and bacteriorhodopsin in small, sonicated vesicles.[21,22]

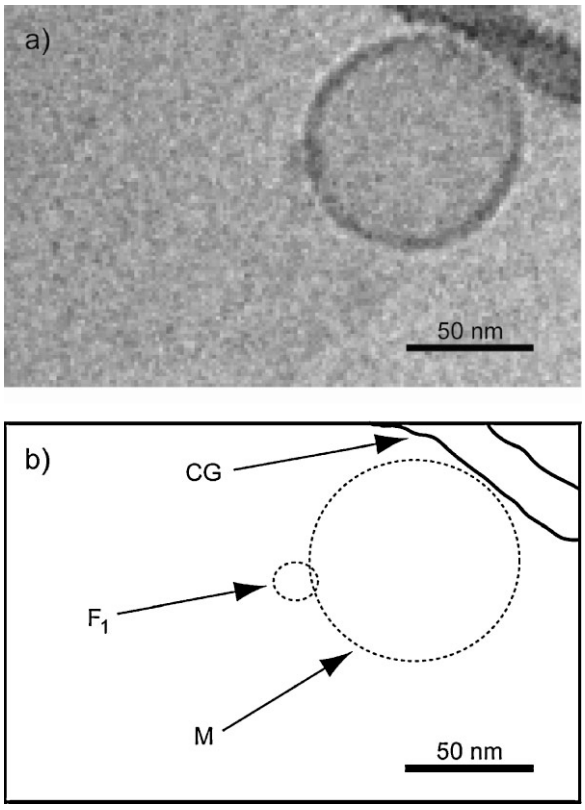

Figure 3. Cryo-electron microscopy image of a proteoliposome with ATP synthase. Here, lipid vesicles were extruded through pores of $r = 50$ nm before protein incorporation. The size of the protrusion at the edge of the liposome (diameter of about 10 nm) coincides with that of the F_1 head group of ATP synthase. The abbreviations are CG for carbon grid, F_1 for F_1 head group and M for membrane.

Cryo Electron Microscopy

Figure 3 represents a cryo electron microscopy image of a proteoliposome incorporating ATP synthase. Here, ATP synthase was incorporated to liposomes extruded through a filter with a pore radius of 50 nm. Although electron microscopy merely yields the projection of the liposomes in the image plane,[38] the size of other proteoliposomes we observed agrees well with that of intact liposomes before protein reconstitution (data not shown). Moreover, as indicated by an arrow, a small protrusion with a diameter of about 10 nm was found to stick out of the liposome membrane. The diameter of the protrusion agrees well with the head group of F_1 ATP synthase, which was reported to be about $\Phi = 10$ nm.[17,39] This suggests that the whole ATP synthase complex including the F_1 head group is incorporated in proteoliposomes. Moreover, despite of the poor statistics limited by the technique, almost all the proteins seem to expose their heads to the bulk. From an energetic point of view, it sounds reasonable that the incorporation of such a highly asymmetric protein occurs from the more compact cytoplasmic domain, but not from the bulkier, hydrophilic F_1 head entity.

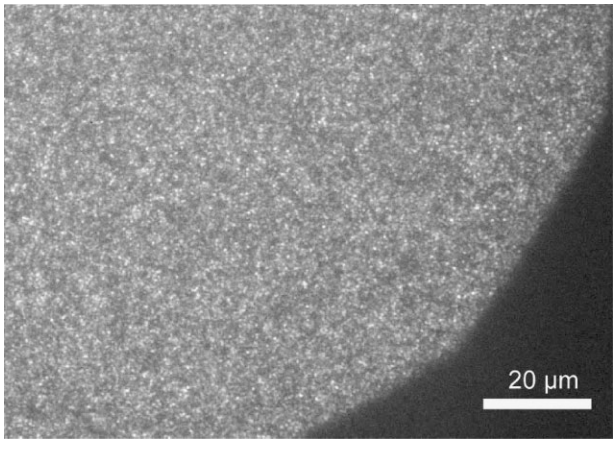

Figure 4. Fluorescence image of a supported membrane doped with ATP synthase labeled with TAMRA directly deposited on a glass slide, resulting in an inhomogeneous fluorescence with numerous defects.

Fluorescence Imaging and Neutron Reflectivity

Figure 4 shows the fluorescence image of a supported membrane doped with TAMRA labeled ATP synthase and

Macromolecular Journals
DOI: 10.1002/mabi.200800128

spread on a bare glass slide. Many fluorescent "spots" and dark patches are clearly visible indicating the presence of numerous local defects, i.e. many proteins are in direct contact with the glass surface and permanently pinned. This problem can be prevented by introducing a polymer layer ("cushion") between the substrate and the membrane.[10] In our case, the cushion consisted of a thin film of regenerated cellulose, which we characterized by neutron reflectivity prior to the spreading of the proteoliposomes (Figure 5). The fitting of the neutron reflectivity curves (Figure 5a) with either a box model (Figure 5b, left) or a combination of a stretched exponential decay profile function and a box model (Figure 5b, right) allowed us to extract the thickness, scattering length density, and root mean square (RMS) roughness of the cellulose layer. The dry layer had a thickness of 4.9 nm and a RMS roughness of 1.7 nm. Although the thickness of a dry film agrees well with one ellipsometry result,[40] the RMS roughness seems to be larger than the value obtained by AFM and X-ray reflectivity,[27] which can be attributed to the longer beam foot print of the neutron beam in an order of several cm^2. It should be noted that the reflectivity data under D_2O can reasonably be interpreted only if the cellulose layer is modeled as two layer: one poorly hydrated layer and the other layer that is highly swollen with D_2O (Figure 5b). The presence of the poorly hydrated layer is attributed to the fact that the HCl vapor could not reach the most buried parts of TMSC during the regeneration process. The swelling of the cellulose in D_2O was modeled by using a stretched exponential decay profile function that accounts for a gradient in the scattering length density along the *z* axis (Figure 5b, right).

When proteoliposomes doped with 1 mol-% of fluorescent lipids (NBD-PC) were spread onto such swollen cellulose films in water, we could observe the formation of a homogeneous and continuous supported lipid membrane over the glass slide (Figure 6a). Lateral distribution of ATP synthase in the polymer-supported membrane was checked by spreading proteoliposomes incorporating prelabeled ATP synthase on the same cellulose support, confirming the homogeneous distribution of proteins (Figure 6b). Thus, these experiments suggest that the hydrated cellulose "cushions" significantly reduce the frictional coupling between proteins and solid surfaces, leading to a homogeneous lateral distribution of ATP synthase. This finding agrees well with our previous studies on human platelet integrin receptors, in which we showed that the lateral homogeneity of protein distribution strongly depends on the presence of polymer cushions[12] or tethers.[13] FRAP (fluorescence recovery after photobleaching) experiments demonstrate that most (>90%) of NBD-labeled lipids are freely diffusive in polymer-supported membranes (diffusion constant: $\approx 2\ \mu m^2 \cdot s^{-1}$) (data not shown), but TAMRA-labeled ATP synthase shows no remarkable sign of lateral diffusion. Currently, this finding is attributed to a strong frictional drag exerted upon the bulky transmembrane F_0 unit (diameter $\approx$ 5 nm) that leads to a significantly small diffusion constant.[14]

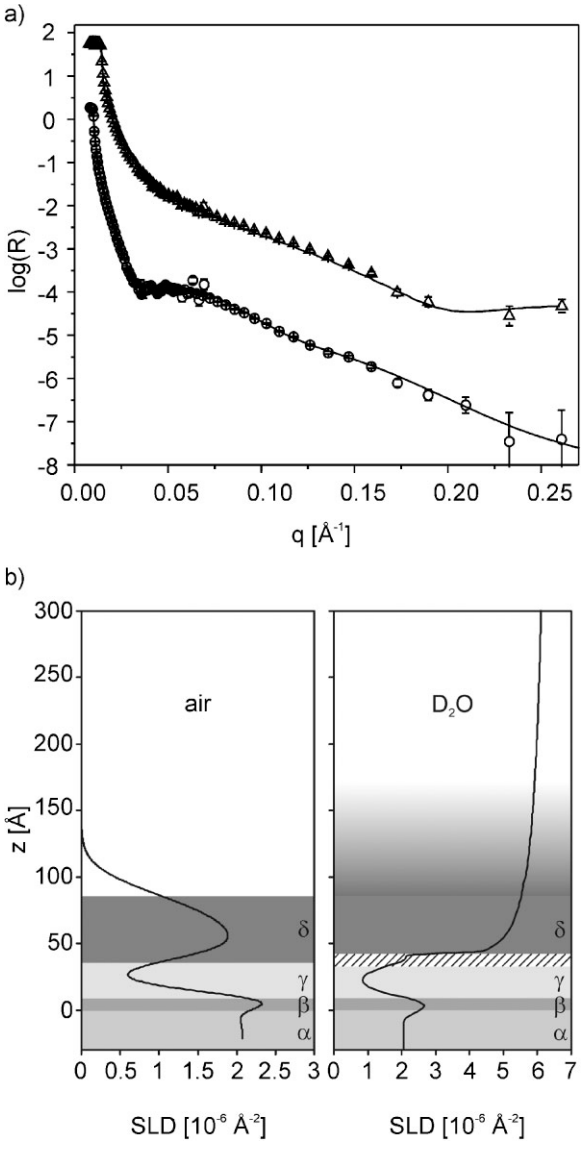

Figure 5. Neutron reflectivity of a regenerated cellulose film, prepared by depositing 10 layers of TMSC onto a hydrophobized silicon block. a) Neutron reflectivity curves of a dry cellulose film (open circles) and the same cellulose film in D_2O (open triangles). The curve in D_2O was translated vertically for clarity. The solid lines correspond to the best fit result models shown in panel b). b) The solid lines correspond to the vertical scattering length density (SLD) profile of the samples. α: silicon block; β: SiO_2; γ: ODTMS; δ: cellulose. Note that the additional dashed box on the right had to be introduced to achieve the best fit and it is due to cellulose layers with different degrees of hydration. The layer corresponding to the hydrated cellulose (δ) was fitted by using a stretched exponential decay profile function.

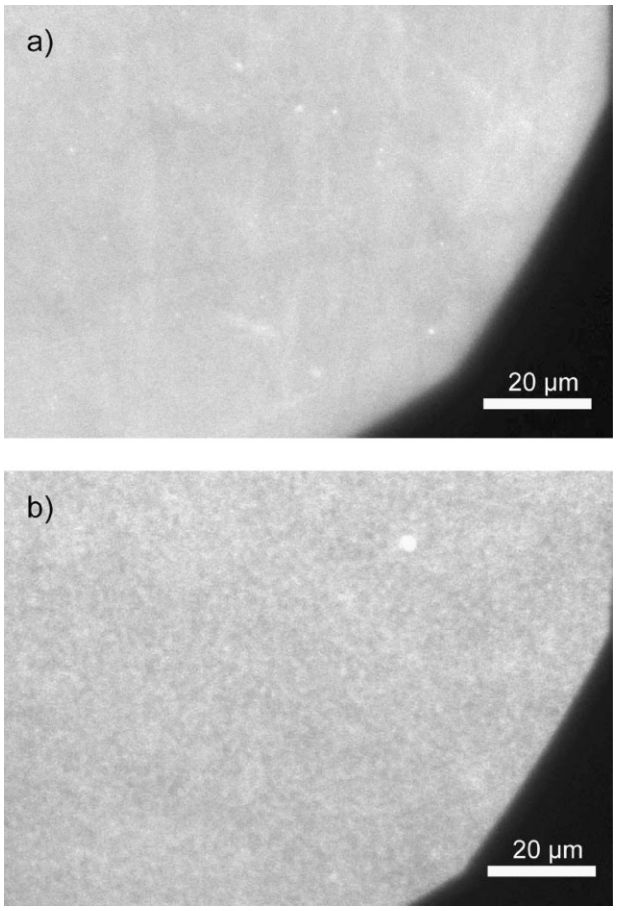

Figure 6. a) Fluorescence image of a supported membrane with 1 mol-% of fluorescent lipids (NBD-PC), deposited on a cellulose film, verifying the homogeneous spreading of the membrane. b) Fluorescence image of a supported membrane with ATP synthase labeled with TAMRA on the same cellulose film, confirming that transmembrane ATP synthase is uniformly distributed over the whole surface.

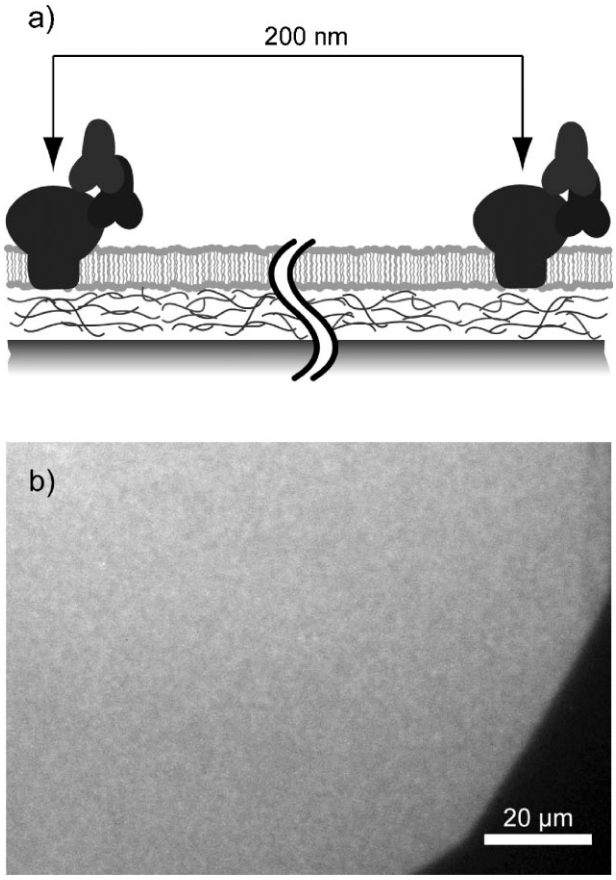

Figure 7. a) Scheme of immuno-fluorescence labeling of ATP synthase incorporated into a polymer supported lipid membrane. The protein was labeled with a first monoclonal antibody against the ATP binding site of the F_1 head group and than with a second FITC conjugated polyclonal antibody. b) Immuno-fluorescence image of ATP synthase in a polymer supported membrane. The homogeneous immuno-fluorescence signal demonstrates that the whole ATP synthase (transmembrane F_o domain, F_1 motor head, and the connecting b and γ subunits) can be reconstituted in a polymer supported membrane, exposing its F_1 head group.

After having demonstrated the incorporation of ATP synthase in proteoliposomes and the possibility of obtaining homogeneous planar membranes from spreading the latter onto cellulose cushions, the next questions that need to be addressed are: (i) whether multiple subunits of ATP synthase are assembled in the supported membrane, and (ii) which orientation (right-side-up or right-side-down) ATP synthase takes in the supported membrane. To answer these open questions, we carried out immuno-fluorescence labeling of ATP synthase. By choosing the monoclonal antibody that binds to the ATP binding site, one can selectively label ATP synthase that exposes its F_1 head group to the bulk buffer (Figure 7a). Since a whole ATP synthase complex consists of a transmembrane F_0 part containing 15 subunits and a catalytic active F_1 head group containing 9 subunits that are connected via the γ subunit,[39] a positive immuno-fluorescence signal would verify the existence of the whole ATP synthase molecule in the supported lipid membrane. As presented in Figure 7b, the homogeneous immuno-fluorescence image confirms that ATP synthase in the supported membrane retains its natural complex structure. Although an antibody that identifies the cytoplasmic domain of ATP synthase is currently not available, the proteins taking right-side-up orientation are uniformly distributed in the supported membrane. Therefore, it is plausible to conclude that mono-dispersive proteoliposomes incorporating transmembrane ATP synthase in a right-side-out orientation are spread over cellulose supports, exposing their outside to the bulk buffer. The

Macromol. Biosci. **2008**, *8*, 1034–1043

Macromolecular Journals

DOI: 10.1002/mabi.200800128

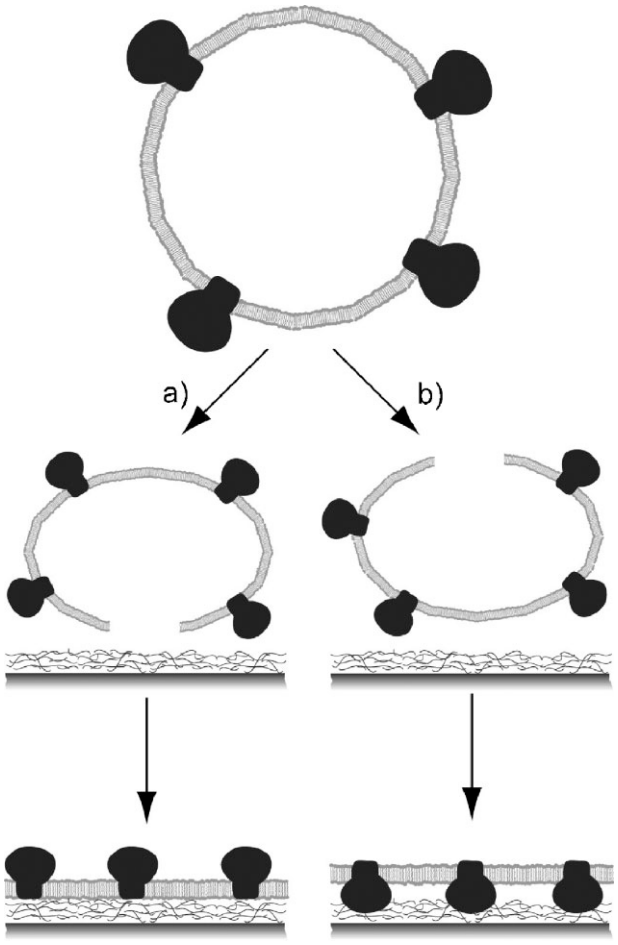

Figure 8. Two possible mechanisms of the fusion of proteoliposomes on polymer supports suggested a) for small vesicles ($\varnothing < 100$ nm) and b) for giant vesicles and ghost cells ($\varnothing > 1$ μm).

mechanism suggested from our experiments (Figure 8a) is consistent with previous studies on supported membranes prepared by the spreading of proteoliposomes doped with photosynthetic reaction centers and tissue growth factor.[41,42] However, this seems to be opposite to that suggested from previous studies on spreading giant lipid vesicles[43] and human red blood cell ghost membranes where the "inside (cytoplasmic domain)" of the membrane is exposed to the bulk (Figure 8b).[28,44] Such a difference in the final protein orientation in supported membranes suggest that the effective contact curvatures between shells and planar supports, i.e. the size difference between proteoliposomes ($\Phi \approx 50$ nm) and cells ($\Phi \approx 5$ μm), would affect the mechanism of membrane rupture. Thus, the spreading of proteoliposomes with a defined protein orientation and different sizes would enable us to clarify the influence of contact curvatures on the resulting membrane orientation. Furthermore, the fact that the monoclonal antibody binds to the catalytic ATP binding site guarantees that the structure of the catalytic activity site is not denatured.

AFM

As additional supporting evidence, we measured the surface topography of the polymer-supported membrane with AFM in contact mode. The topographic surface profile (Figure 9a) clearly indicates the presence of uniformly distributed protrusions on a smooth membrane surface (RMS roughness = 1.2 nm). Such protrusions could not be found on pure lipid membranes without proteins on the same polymer support (data not shown). The height of the protrusions of 7–9 nm (Figure 9b) agrees well with the diameter of the F_1 head group ($\Phi \approx 10$ nm). Moreover, the characteristic lateral length scale of protrusions obtained from topographic profiles (≈30 nm) seems reasonable, if one considers the distortion of the topographic profile of spherical objects (like F_1 head groups) by AFM scans.[a] Furthermore, the lateral density of protrusions (center-to-center distance: 180 nm) agrees well with the expected center-to-center distance between neighboring ATP synthase, as calculated from the molar ratio of lipids and proteins (140 nm).

Conclusion

Lipid and protein concentrations in proteoliposomes determined after the size exclusion chromatography proved the incorporation of ATP synthase in lipid vesicles. DLS (Figure 2) showed no detectable change in the size histograms before and after the protein incorporation, confirming that proteins are transferred from TDOC micelles into phospholipid vesicles without disruption of lipid membranes. Electron microscopy images (Figure 3) suggested that ATP synthase is incorporated into membranes from the more "compact" cytoplasmic side but not from the "bulkier" F_1 head group, which energetically seems reasonable by considering the highly asymmetric structure of ATP synthase. Such a "right-side-out" orientation was also implied by immuno-fluorescence labeling of proteoliposomes (data not shown), although the "negative" test is not possible due to the fact that the site specific antibody to the cytoplasmic domain is currently not

[a] If one assumes a spherical object, the lateral length size of the object L can be related to the FWHM of the topographic profile and the radius of the tip r *by* $\mathrm{FWHM} = 2\sqrt{rL + L^2/4}$.[45] Though the tip radius provided by the manufacturer might be erroneous, the values roughly estimated from the measured FWHM ($L = 5$–10 nm) seem reasonable.

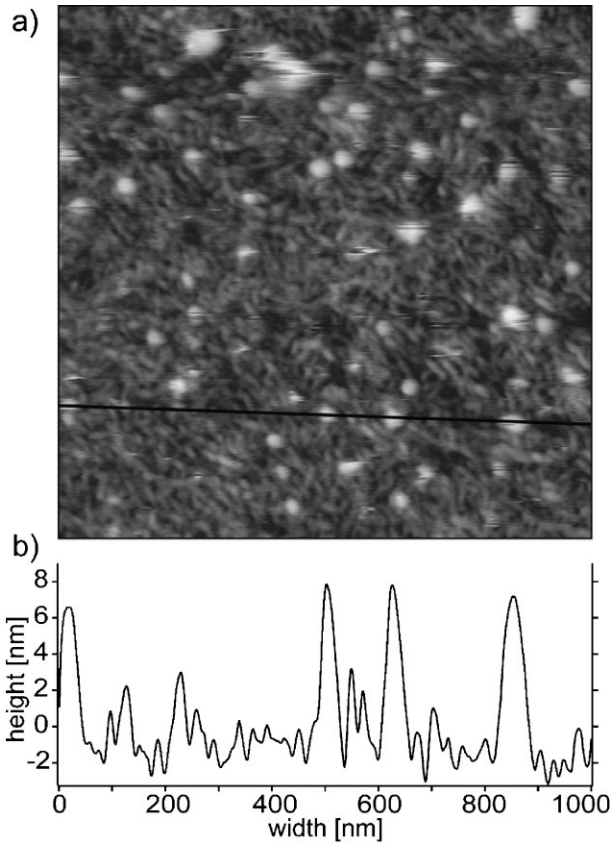

Figure 9. a) AFM topographic image of a supported membrane with ATP synthase on a cellulose film (scan area: $1 \times 1\ \mu m^2$). The full range of the color code coincides with the height difference of 10 nm. The height of the protrusions obtained from the height profile (b) is reasonable from the size of the F_1 head group of ATP synthase. Furthermore, the lateral density of the protrusions calculated from 120 measurements (180 nm average distance) agreed well with the one expected from the protein molar fraction (140 nm average distance).

available. Though further studies will be necessary to unravel the influence of vesicle sizes on the membrane orientation, both immuno-fluorescence images and surface topography of the polymer-supported membrane indicate that ATP synthase exposes its F_1 head groups to the bulk buffer. The strategy we demonstrated in this paper can be adopted for other transmembrane proteins, which enables us to evaluate in a quantitative manner the function of individual proteins in the supported membrane system.

Acknowledgements: This work has been supported by the *German Science Foundation* (DFG SFB563), the *Federal Ministry of Education and Science* (BMBF), and the *Fonds der Chemischen Industrie*. We thank *W. Doster* for supporting DLS measurements.

Received: May 16, 2008; Accepted: June 26, 2008; DOI: 10.1002/mabi.200800128

Keywords: biomimetic; membranes; polysaccharides; proteins; surfactants

[1] A. A. Brian, H. M. McConnell, *Proc. Natl. Acad. Sci. USA* **1984**, *81*, 6159.
[2] E. Sackmann, *Science* **1996**, *271*, 43.
[3] J. T. Groves, M. L. Dustin, *J. Immunol. Meth.* **2003**, *278*, 19.
[4] T. H. Watts, H. E. Gaub, H. M. McConnell, *Nature* **1986**, *320*, 179.
[5] T. M. Bayerl, M. Bloom, *Biophys. J.* **1990**, *58*, 357.
[6] S. A. Tatulian, P. Hinterdorfer, G. Baber, L. K. Tamm, *EMBO J.* **1995**, *14*, 5514.
[7] S. Terrettaz, T. Stora, C. Duschl, H. Vogel, *Langmuir* **1993**, *9*, 1361.
[8] C. A. Keller, K. Glasmaester, V. P. Zhdanov, B. Kasemo, *Phys. Rev. Lett.* **2000**, *84*, 5443.
[9] S. J. Johnson, T. M. Bayerl, D. C. McDermott, G. W. Adam, A. R. Rennie, R. K. Thomas, E. Sackmann, *Biophys. J.* **1991**, *59*, 289.
[10] M. Tanaka, E. Sackmann, *Nature* **2005**, *437*, 656.
[11] M. Tanaka, *MRS Bull.* **2006**, *31*, 513.
[12] S. Goennenwein, M. Tanaka, B. Hu, L. Moroder, E. Sackmann, *Biophys. J.* **2003**, *85*, 846.
[13] O. Purrucker, A. Foertig, R. Jordan, M. Tanaka, *Chem. Phys. Chem.* **2004**, *5*, 327.
[14] O. Purrucker, A. Foertig, R. Jordan, E. Sackmann, M. Tanaka, *Phys. Rev. Lett.* **2007**, *98*.
[15] O. Purrucker, S. Goennenwein, A. Foertig, R. Jordan, M. Rusp, M. Barmann, L. Moroder, E. Sackmann, M. Tanaka, *Soft Matter* **2007**, *3*, 333.
[16] O. Purrucker, A. Foertig, K. Ludke, R. Jordan, M. Tanaka, *J. Am. Chem. Soc.* **2005**, *127*, 1258.
[17] T. Nawroth, H. Conrad, K. Dose, *Physica B* **1989**, *156–157*, 477.
[18] P. D. Boyer, *Annu. Rev. Biochem.* **1997**, *66*, 717.
[19] P. D. Boyer, *J. Biol. Chem.* **2002**, *277*, 39045.
[20] J. Weber, *Trends Biochem. Sci.* **2007**, *32*, 53.
[21] G. Gruber, J. Godovac-Zimmermann, T. Nawroth, *Biochim. Biophys. Acta* **1994**, *1186*, 43.
[22] H.-J. Freisleben, K. Zwicker, P. Jezek, G. John, A. Bettin-Bogutzki, K. Ring, T. Nawroth, *Chem. Phys. Lipids* **1995**, *78*, 137.
[23] Y.-S. Chung, M. R. J. Salton, *Microbios* **1988**, *54*, 187.
[24] B. Hu, D. Finsinger, K. Peter, Z. Guttenberg, M. Barmann, I. Kessler, A. Escherich, L. Moroder, J. Bohm, W. Baumeister, S. F. Sui, E. Sackmann, *Biochemistry* **2000**, *39*, 12284.
[25] K. Zwicker, Ph.D. Thesis, University of Mainz 1992.
[26] H. Hillebrandt, M. Tanaka, E. Sackmann, *J. Phys. Chem. B* **2002**, *106*, 477.
[27] M. Schaub, G. Wenz, G. Wegner, A. Stein, D. Klemm, *Adv. Mater.* **1993**, *5*, 919.
[28] M. Tanaka, S. Kaufmann, J. Nissen, M. Hochrein, *Phys. Chem. Chem. Phys.* **2001**, *3*, 4091.
[29] R. Cubitt, G. Fragneto, *Appl. Phys. A. – Mater. Sci. Process.* **2002**, *74*, S329.
[30] A. Nelson, *J. Appl. Crystallogr.* **2006**, *39*, 273.
[31] L. G. Parratt, *Phys. Rev.* **1954**, *95*, 359.
[32] S. W. Provencher, *Comp. Phys. Comm.* **1982**, *27*, 229.
[33] O. L. Krivanek, S. L. Friedman, A. J. Gubbens, B. Kraus, *Ultramicroscopy* **1995**, *59*, 267.
[34] A. De Jong, J. Rees, W. Busing, U. Lucken, *Prog. Biophys. Mol. Biol.* **1996**, *65*, 194.

DOI: 10.1002/mabi.200800128

[35] C. H. Fiske, Y. Subbarow, *J. Biol. Chem.* **1925**, *66*, 375.
[36] A. Neidhardt, T. Nawroth, M. Huetsch, K. Dose, *FEBS Lett.* **1991**, *280*, 179.
[37] B. A. Korgel, J. H. van Zanten, H. G. Monbouquette, *Biophys. J.* **1998**, *74*, 3264.
[38] S. U. Egelhaaf, E. Wehrli, M. Muller, M. Adrian, P. Schurtenberger, *J. Microsc. (Oxford)* **1996**, *184*, 214.
[39] G. Gruber, *J. Bioenerg. Biomembr.* **2000**, *32*, 341.
[40] F. Rehfeldt, M. Tanaka, *Langmuir* **2003**, *19*, 1467.
[41] P. B. Contino, C. A. Hasselbacher, J. B. A. Ross, Y. Nemerson, *Biophys. J.* **1994**, *67*, 1113.
[42] J. Salafsky, J. T. Groves, S. G. Boxer, *Biochemistry* **1996**, *35*, 14773.
[43] J. Radler, H. Strey, E. Sackmann, *Langmuir* **1995**, *11*, 4539.
[44] M. Tanaka, A. P. Wong, F. Rehfeldt, M. Tutus, S. Kaufmann, *J. Am. Chem. Soc.* **2004**, *126*, 3257.
[45] A. Engel, C. A. Schoenenberger, D. J. Muller, *Curr. Opin. Struct. Bio.* **1997**, *7*, 279.